Programmed cell death during the transition from multicellular structures to globular embryos in barley androgenesis

Maraschin, S. de F.; Gaussand, G.M.D.J.; Pulido, A.; Olmedilla, A.; Lamers, G.E.; Korthout, H.A.; ... ; Wang, M.

Planta (2005) 221: 459–470
DOI 10.1007/s00425-004-1460-x

ORIGINAL ARTICLE

**Simone de F. Maraschin · Gwénaël Gaussand
Amada Pulido · Adela Olmedilla · Gerda E. M. Lamers
Henrie Korthout · Herman P. Spaink · Mei Wang**

Programmed cell death during the transition from multicellular structures to globular embryos in barley androgenesis

Received: 7 July 2004 / Accepted: 12 November 2004 / Published online: 12 January 2005

Abstract Androgenesis represents one of the most fascinating examples of cell differentiation in plants. In barley, the conversion of stressed uninucleate microspores into embryo-like structures is highly efficient. One of the bottlenecks in this process is the successful release of embryo-like structures out of the exine wall of microspores. In the present work, morphological and biochemical studies were performed during the transition from multicellular structures to globular embryos. Exine wall rupture and subsequent globular embryo formation were observed only in microspores that divided asymmetrically. Independent divisions of the generative and the vegetative nuclei gave rise to heterogeneous multicellular structures, which were composed of two different cellular domains: small cells with condensed chromatin structure and large cells with normal chromatin structure. During exine wall rupture, the small cells died and their death marked the site of exine wall rupture. Cell death in the small cell domain showed typical features of plant programmed cell death. Chromatin condensation and DNA degradation preceded cell detachment and cytoplasm dismantling, a process that was characterized by the formation of vesicles and vacuoles that contained cytoplasmic material. This morphotype of programmed cell death was accompanied by an increase in the activity of caspase-3-like proteases. The orchestration of such a death program culminated in the elimination of the small generative domain, and further embryogenesis was carried out by the large vegetative domain. To date, this is the first report to show evidence that programmed cell death takes part in the development of microspore-derived embryos.

Keywords Androgenesis · Barley · Caspase-3 like proteases · Exine wall · Programmed cell death · TUNEL

Abbreviations MCS: Multicellular structure inside the exine wall · ELS: Embryo-like structure released out of the exine wall · PCD: Programmed cell death · TUNEL: Terminal deoxynucleotidyl transferase-mediated dUTP nick end labelling · FDA: Fluorescein-diacetate

S. F. Maraschin (✉) · G. Gaussand · M. Wang
Center for Phytotechnology LU/TNO, Leiden University, Wassenaarseweg 64, 2333 AL Leiden, The Netherlands
E-mail: maraschin@rulbim.leidenuniv.nl
Tel.: +31-71-5274909
Fax: +31-71-5274999

A. Pulido · A. Olmedilla
Departamento de Bioquímica, Biología Celular y Molecular de Plantas, Estación Experimental del Zaidín, Consejo Superior de Investigaciones Científicas, Granada, Spain

H. Korthout · M. Wang
TNO Department of Applied Plant Sciences, Zernikedreef 9, P.O. Box 2215, 2301 CE Leiden, The Netherlands

G. E. M. Lamers · H. P. Spaink
Institute of Biology Leiden, Leiden University, Wassenaarseweg 64, P.O. Box 9505, 2300 RA Leiden, The Netherlands

Introduction

The life cycle of flowering plants alternates the dominant diploid sporophytic phase with the short-lived, small-sized structures of the haploid female and male gametophytes, represented by the embryo sac and pollen grains. Microspores, or young pollen grains, have the remarkable ability of switching from their normal gametophytic development towards a sporophytic route. This fascinating example of phase transition during the alternation of generations in plants is called androgenesis (Raghavan 1986). Androgenesis can be efficiently triggered in several plant species by means of stress treatment around the first pollen mitosis. Androgenic microspores under specific culture conditions are capable of forming multicellular structures (MCSs), which differentiate into embryo-like structures (ELSs) (Touraev et al. 1997). The successive ELS developmental stages are known to parallel somatic and zygotic

embryogenesis, providing advantages for both fundamental and applied research (Wang et al. 2000).

The initial steps of microspore embryogenesis are, however, unusual to any other embryogenic system, since MCS formation takes place inside the exine wall of microspores (Mordhorst et al. 1997). During the initial phase of microspore embryogenesis, several patterns of cell division have been identified to take place inside the exine wall. The asymmetric division of the microspore nucleus resulting in a generative and a vegetative cell characterizes the A-pathway. In the A-pathway, MCSs are formed from repeated divisions of the vegetative cell, while the generative cell or its derivatives degenerate and die (Sunderland 1974). This is the most widely spread mechanism of MCSs formation during androgenesis and it has been described in several plant species, including most cereals (Raghavan 1986). In the B-pathway, it is the symmetric division of the microspore nucleus that gives rise to MCSs (Sunderland 1974). The B-pathway is known to play a major role in rapeseed (*Brassica napus* L.), potato (*Solanum tuberosum* L.), tobacco (*Nicotiana tabacum* L) and wheat (*Triticum aestivum* L.) microspore embryogenesis (Zaki and Dickinson 1991; Říhová and Tupý 1999; Touraev et al. 1996; Indrianto et al. 2001), and it has also been described among barley MCSs (Sunderland and Evans 1980). An alternative route to androgenesis is defined by the independent divisions of the generative and vegetative cells, giving rise to MCSs with heterogeneous compositions. This modified version of the A-pathway, also termed E-pathway (Raghavan 1986), has been described in barley, maize, tobacco and pepper (*Capsicum annum* L.) MCSs (Sunderland et al. 1979; Pretova et al. 1993; Touraev et al. 1996; Kim et al. 2004). In contrast to the known A- and B-pathways, in which the roles of the generative and vegetative cells are clearer, in this modified version of the A-pathway, both generative and vegetative cells appear to contribute equally to embryo formation (Raghavan 1986).

What leads microspores to give preference to a particular division sequence is not yet clear. Different developmental pathways have been reported to vary according to plant species, and in response to different stress treatments and the microspore developmental stage (Raghavan 1986; Sunderland et al. 1979; Říhová and Tupý 1999; Kasha et al. 2001; Kim et al. 2004). In barley, a model species for androgenesis studies, a correlation between the yield of ELSs and the presence of heterogeneous MCSs has been reported in anther cultures of cold-stressed spikes (Sunderland and Huang 1985). Nevertheless, no link has been established between the microspore developmental pathways that ultimately lead to barley ELSs formation. Recently, the development of mannitol-stressed barley microspores into ELSs has been monitored by time-lapse tracking (Maraschin et al. 2004). Following osmotic and starvation stress, 50% of the microspores were triggered to divide and to form MCSs; however, only 20% of the MCSs further developed into ELSs. The development of ELSs was conditioned to a specific type of MCSs that released ELSs characteristically at the opposite side of the pollen germ pore, a process that was marked by the death of the cells situated at the exine wall rupture. The elimination of a specific cell type during the transition phase from MCSs to ELSs suggests that this might be an active cell death process. Programmed cell death (PCD) is a genetically programmed process of cell death that occurs during development and in response to environmental triggers in a wide variety of biological systems, including higher plants (Raff 1998; Lam 2004). Despite the nature of the PCD signal, animal and plant cells undergoing PCD show several common cytological features that include activation of specific proteases, condensation of chromatin, DNA cleavage into ~180 bp internucleosomal fragments and loss of cell shape and integrity (Pennel and Lamb 1997). In animal cells, PCD is regulated by a conserved family of cysteine proteases that specifically cleave target proteins after an Asp residue. The most prevalent executioner caspase in animal cells is caspase-3 (Thornberry and Lazebnik 1998). Although caspase-3 proteases have not been yet identified in plants, caspase-3-like activity towards the synthetic fluorogenic caspase-3 substrate *N*-acetyl-DEVD-7-amino-4-methylcoumarin (Ac-DEVD-AMC) has been described and related to PCD (Korthout et al. 2000; Lam and del Pozo 2000).

In order to investigate whether PCD takes place during the transition from MCSs into ELSs, biochemical and morphological markers for PCD were assayed. During the transition of MCSs into ELSs, the death of the cells at the site of rupture was used as a marker for embryogenic development. With the help of this marker, the developmental pathways that lead to ELS formation during barley androgenesis were investigated. Our results indicate that embryogenic MCSs are formed by the modified A-pathway, and therefore are composed of two different cellular domains, displaying generative and vegetative characteristics. During exine wall rupture, the small cell domain derived from the generative cell was eliminated by PCD, while the large cell domain derived from the vegetative cell contributed to globular embryo formation. This is the first report to show that PCD takes place during the transition from MCSs into ELSs in barley androgenesis.

Materials and methods

Androgenesis induction and microspore culture

Donor plants of barley (*Hordeum vulgare* L. cv Igri, Landbouw Bureau Wiersum, The Netherlands) were grown in a phytotron under conditions described previously (Hoekstra et al. 1992). Pre-treatment consisted of incubation of anthers containing mid-late to late uninucleate microspores in 0.37 M mannitol solution for 4 days in the dark, at 25°C (Hoekstra et al. 1992). After pre-treatment, microspores were isolated as described previously (Maraschin et al. 2003, 2004). The enlarged

microspores were plated in medium I (Hoekstra et al. 1992) at a density of 2.10^4 enlarged microspores. ml^{-1} and cultured for 0–14 days for MCS and ELS development (Hoekstra et al. 1993). Cultures were sieved through appropriate nylon mesh sizes and dividing MCSs and ELSs were collected as previously described (Maraschin et al. 2003).

DAPI staining of nuclei

Nuclear evolution of isolated-microspore cultures was followed by 4′,6-diamidino-2-phenylindole (DAPI) staining (Vergne et al. 1987). Fresh MCSs were briefly fixed in Carnoy (70% ethanol: acetic acid, 3:1, v/v), after which they were rinsed in 70% (v/v) ethanol and stained for 10 min in 1 $mg{\cdot}ml^{-1}$ DAPI aqueous solution containing 1% (v/v) Triton X-100. Squashed material was studied under UV light with a Zeiss Axioplan microscope.

Cell viability and cell-death staining of MCSs

Multicellular structures and ELSs at different stages of culture were stained for cell death with Sytox orange (Molecular Probes) and for cell viability with fluorescein-diacetate (FDA, Sigma) as described previously (Maraschin et al. 2004). MCSs were observed using a Leica DM IRBE confocal microscope. An argon (488 nm) and a krypton (568 nm) laser were used for visualization of the FDA (Ex 488 nm, Em 502-540) and the Sytox orange (Ex 568, Em 570-610) signals, respectively. The percentage of ELSs released out of the exine wall was determined in three ($n = 3$) independent experiments by estimating the relative amount of ELSs which showed FDA/Sytox orange positive domains within 300 MCSs per experiment (Maraschin et al. 2004).

Terminal deoxynucleotidyl transferase-mediated dUTP nick end labelling

Multicellular structures and ELSs from different developmental stages were fixed in 2% (w/v) glutaraldehyde in 10 mM NaH_2PO_4, 120 mM NaCl, 2.7 mM KCl, pH 7.4 (phosphate-buffered saline, PBS) overnight at room temperature. After dehydration at room temperature in a graded series of 70%, 90%, 96% and 100% (v/v) ethanol, samples were embedded in Technovit (Heraeus Kulzer). Sections (2 μm) were attached on Biobond (Biocell) coated slides. Terminal deoxynucleotidyl transferase-mediated dUTP nick end labelling (TUNEL) assay was done using an in situ cell death detection kit (Roche) according to the manufacturer's instructions. Following TUNEL reaction, cross-sections were stained with Sytox orange for visualization of nuclei (Maraschin et al. 2004). Samples were observed using a Zeiss Axioplan confocal microscope with a MRC 1024 ES Biorad module. An argon–krypton laser (488–568 nm) was used for the visualization of the TUNEL (Ex 488 nm, Em 522 DF 32) and the Sytox orange (Ex 568, Em 605 DF 32) signals.

DNA isolation and electrophoresis

Genomic DNA was isolated from MCSs and ELSs from different developmental stages that were frozen in liquid nitrogen immediately after sampling. Samples were ground with a mortar and pestle to a fine powder and DNA was isolated as described previously (Wang et al. 1999). Five micrograms of genomic DNA/lane were separated on a 2% (w/v) agarose gel containing 1% (w/v) ethidium bromide in 0.2 M Tris-acetate, 0.05 M EDTA pH 8.3 at 50 V for 4 h, along with a Smart DNA ladder (Eurogentec).

Protein isolation and caspase-3-like assay

Multicellular structures and ELSs at different time points of culture were frozen in liquid nitrogen and were used to obtain cytosolic protein extracts. Samples were ground in 500 μl ice-cold extraction buffer containing 100 mM HEPES (pH 7.2), 10% (w/v) sucrose, 0.1% (w/v) CHAPS, 5 mM DTT and 10^{-6}% (v/v) NP40 using a glass mortar and pestle. Subsequently, the homogenate was incubated on ice for 15 min and centrifuged two times for 10 min at 13,000 rpm at 4°C to pellet cell debris. The supernatant was cleared by filtration over a 0.22 μm Millex syringe driven filter unit (Millipore). For in vitro caspase-3-like activity, 75 μl of cytosolic extracts containing 5 μg of proteins were mixed to 25 μl of the synthetic fluorogenic caspase-3 substrate *N*-acetyl-DEVD-7-amino-4-methylcoumarin (Ac-DEVD-AMC, 75 μM) or with a mix of caspase-3 substrate Ac-DEVD-AMC and inhibitor (Ac-DEVD-CHO, 250 μM). The measurements were performed every 10 min for 2 h at room temperature in triplicates for each sample in three independent experiments ($n = 3$). Substrate cleavage was detected in a Perkin Elmer fluorescence spectrometer LS50B at an excitation wavelength of 380 nm and an emission wavelength of 460 nm. The standard setting used an excitation and an emission slit value of 5.0. Kinetics of substrate hydrolysis was tested to be linear throughout the 2 h reactions.

Transmission electron microscopy

Multicellular structures and ELSs fixation, dehydration and embedding procedures were performed as described previously (Maraschin et al. 2004). Ultrathin sections were made using an ultramicrotome (Ultracut, Leica), stained for 10 min in 2% (w/v) uranyl acetate in 50% (v/v) ethanol, and for 10 min in 0.4% (w/v) lead citrate, followed by thorough washes in deionized filtered water. Electron micrographs were made using a Jeol 100 CX

electron microscope. Pictures were taken at 60 kV on a FGP- film (Kodak 5302).

Scanning electron microscopy

Multicellular structures and ELSs from different developmental stages were fixed in a mixture of 2% (w/v) paraformaldehyde and 2.5% (v/v) glutaraldehyde in 0.1 M sodium cacodylate buffer, pH 7.3, for 3 h at room temperature. Samples were dehydrated through a graded series of 50%, 70%, 90%, 96% and 100% (v/v) acetone and dried using a Bal-Tec CPD 030 critical point drier. The samples were then mounted on stubs, coated with gold on a Polaron SEM coating unit E5100 and observed using a Jeol 6400 scanning electron microscope.

Experimental data

Data presented on morphological analysis of developing MCSs were representative of at least 300 MCSs observed per time point in three independent experiments ($n = 3$). Mean values ± SD of the daily frequencies of exine wall rupture were calculated as percentages. Significance of the differences in mean values of the specific caspase-3-like activities was tested with a Student's *t*-test.

Results

Mannitol treatment induces the formation of homogeneous and heterogeneous MCSs with different fates in culture

In order to investigate the developmental pathways by which mannitol-treated barley microspores develop into MCSs, the degree of DNA condensation in the nucleus was used as a marker to distinguish cells with vegetative and generative origins (Sunderland 1974). During pollen and androgenic development, the generative cells are located opposite the germ pore at the edge of the structure, connected to the intine (Huang 1986; Sunderland et al. 1979). On the first day of culture, DAPI nuclear staining revealed that both symmetric and asymmetric divisions characterized the initial phase of MCSs formation. While symmetric divisions gave rise to two nuclei with normal chromatin structure (Fig. 1a), asymmetric divisions gave rise to two nuclei with different degrees of chromatin structure (Fig. 1b). In asymmetrically dividing microspores, the small nucleus with intense DAPI staining indicates the generative cell, and the large nucleus with weaker DAPI staining indicates the vegetative cell. Based on these DAPI-staining properties, MCSs with both homogeneous and heterogeneous nuclei composition were observed in 3-day-old

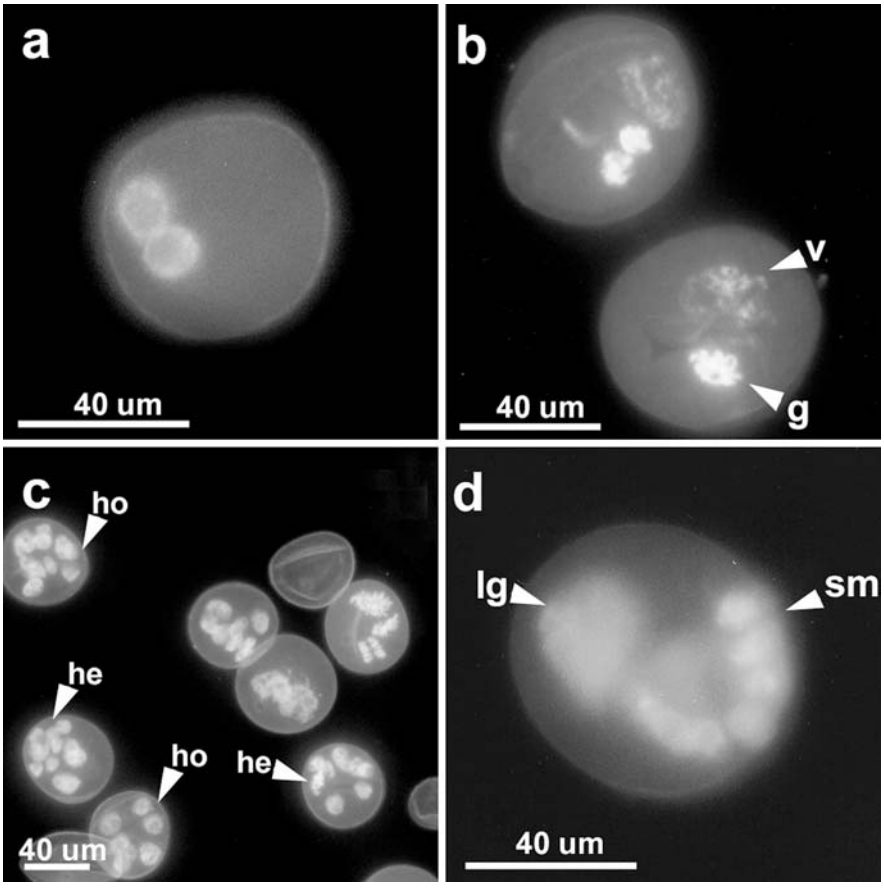

Fig. 1 DAPI staining of nuclei in the first days of culture. **a**, **b** Enlarged microspores at the first day of culture illustrating symmetric and asymmetric division of nuclei. **c**, **d** Three-day-old MCSs with homogeneous and heterogeneous composition. *g* Generative nucleus, *lg* large nuclei with normal chromatin structure, *he* heterogeneous, *ho* homogenous, *sm* small condensed nuclei, *v* vegetative nucleus

cultures (Fig. 1c, indicated by arrows). A close-up of heterogeneous MCSs shows that the small, condensed nuclei formed a file at the edge of the exine wall. The degree of chromatin condensation and the position at the edge of the exine wall point out their generative cell origin. At this stage, they divided more frequently than the large nuclei (Fig. 1d).

To better understand the morphology and the fate of the homogeneous and heterogeneous MCSs during the transition phase between MCSs and ELSs, cross-sections of homogeneous and heterogeneous MCSs were analyzed using differential interference contrast (DIC) microscopy and Sytox orange nuclear staining. Prior to exine wall rupture, 5-day-old homogeneous MCSs were composed of cells of equal size with rounded nuclei (Fig. 2a, b). In contrast, in 5-day-old heterogeneous MCSs, the generative domain was composed of small, compact cells with vermiform nuclei showing condensed chromatin structure and dense cytoplasm, while the vegetative domain was composed of large cells with round nuclei and normal chromatin structure (Fig. 2c, d). At the time of exine wall rupture, 7-day-old homogeneous MCSs appeared shrunken and did not develop further (Fig. 2e, f). Interestingly, only heterogeneous MCSs ruptured the exine wall after 7 days of culture. Heterogeneous MCSs displayed exine rupture exclusively at the domain composed of small cells, opposite to the pollen germ pore (Fig. 2g). At the exine wall rupture site, the small cell domain fell apart, while cell divisions were clearly observed within the large cell domain (Fig. 2h).

During microspore embryogenesis, exine wall rupture has been demonstrated to be accompanied by cell death at the site of rupture (Maraschin et al. 2004). In order to establish a link between the localization of the two different morphological domains in heterogeneous MCSs and the dying cells described previously in embryogenic MCSs, cell viability (FDA) and cell death (Sytox orange) staining were performed around the time of exine wall rupture (Fig. 3a–d). During the transition from MCSs to ELSs in 5- to 7-day-old cultures, Sytox orange-stained cells were located at the edge of the MCSs, at the site of exine wall rupture. This was the same localization as the domain composed of small cells in heterogeneous MCSs with ruptured exine (Fig. 2g, h). This indicates that the small cell domain dies at the time of exine wall rupture. At later stages, a few dead cells were observed at the periphery of 9-day-old ELSs, and in most of the 11-day-old ELSs, they had been completely eliminated (Fig. 3c, d).

Elimination of the small cell domain by PCD during exine wall rupture

The first PCD marker investigated during exine wall rupture was DNA cleavage. Assessment of in situ DNA cleavage was done by TUNEL assay. In liquid cultures, 5-day-old MCS had not yet come out of the exine wall (Fig. 3a). At this stage, some MCSs already showed signs of DNA degradation, as TUNEL-positive nuclei were observed in the small cells with condensed chromatin structure of nuclei. No TUNEL signal was found in the large cell domain (Fig. 3e–h).

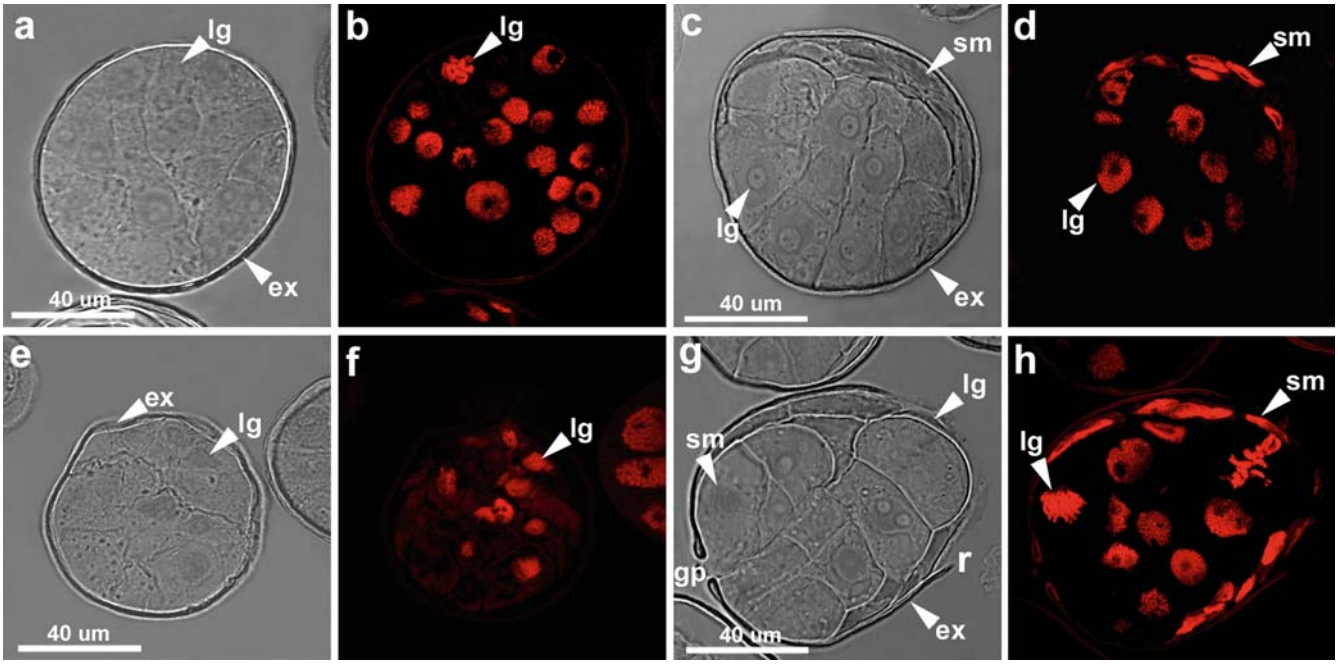

Fig. 2 Cross-sections illustrating morphology of homogeneous and heterogeneous 5- and 7-day-old MCSs visualized by DIC and confocal microscopy stained by Sytox orange. **a**, **b** Homogeneous 5-day-old MCS composed of large cells with round nuclei. **c**, **d** Heterogeneous 5-day-old MCS displaying two cellular domains. **e**, **f** Homogeneous 7-day-old MCS displaying shrinkage at the time of exine wall rupture. **g**, **h** Exine wall rupture in heterogeneous MCS at the site of the small cell domain. *ex* Exine wall, *gp* germ pore, *lg* large cell domain, *r* exine wall rupture, *sm* small cell domain

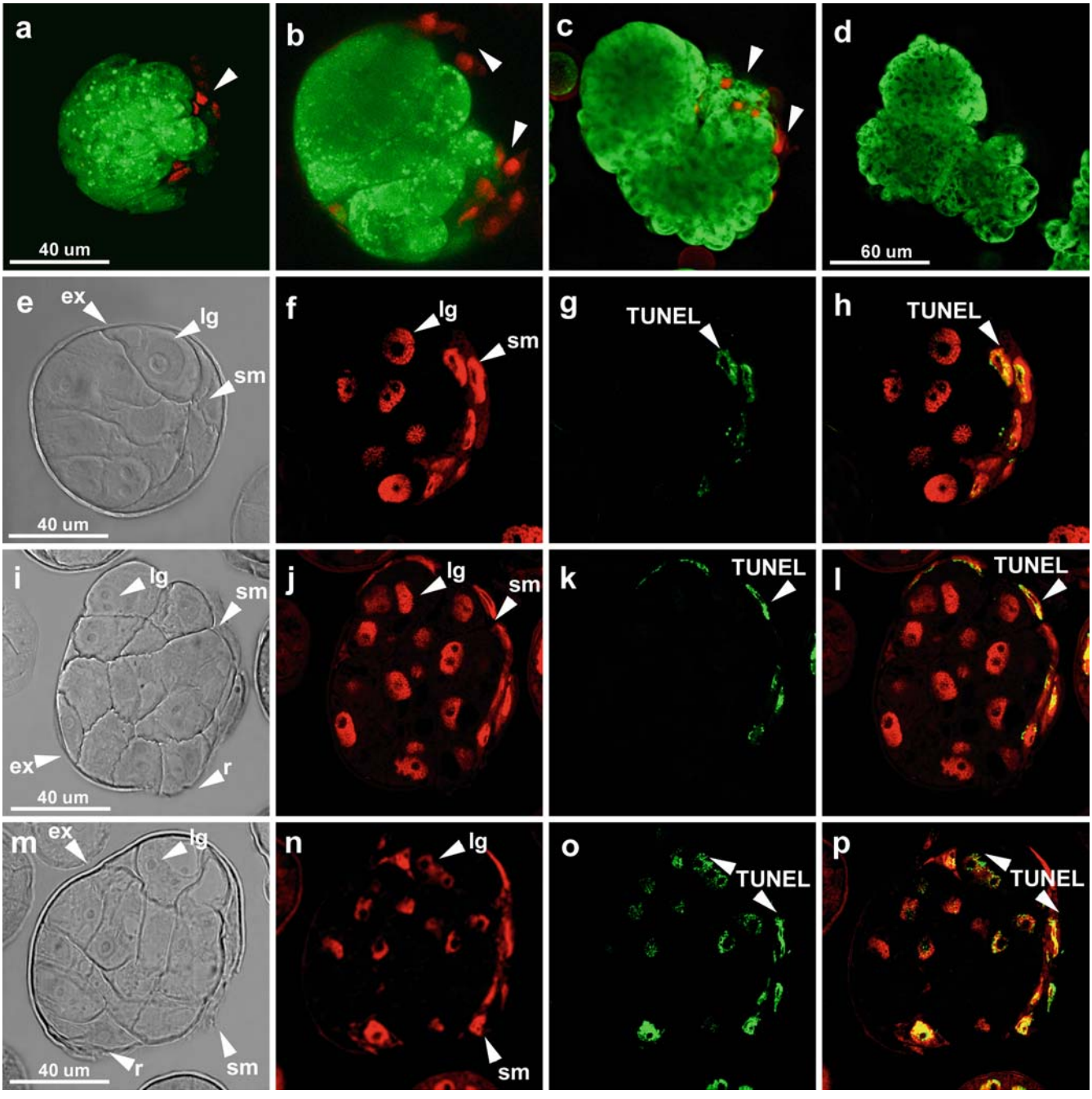

Fig. 3 Fate of the different cellular domains during exine wall rupture visualized by FDA/Sytox orange staining and TUNEL. **a** Five-day-old MCS, **b** 7-day-old MCS, **c** 9-day-old ELS and **d** 11-day-old ELS showing viability of the large cell domain as indicated by FDA staining, whereas the small cells are stained by Sytox orange and are progressively eliminated from the ELS (indicated by *arrows*). **e**–**h** Transmitted light image, Sytox orange nuclear staining and TUNEL signal on cross-sections of 5-day-old MCS and **i**–**l** 7-day-old MCS. **h**, **l** Are merged images of **f**, **g** and **j**, **k**, respectively. **m**–**p** Transmitted light image, Sytox orange nuclear staining and TUNEL signal on a DNase I-treated cross-section of 7-day-old MCS. **p** Is a merged image of **n**, **o**. TUNEL-positive nuclei in the small cell domain are indicated by *arrows*. *ex* Exine wall, *lg* large cell domain, *r* exine wall rupture, *sm* small cell domain

After 7 days of culture, most of the MCSs had already ruptured the exine wall. The small cells appeared attached to the boundaries of the ruptured exine and their nuclei were heavily labelled by TUNEL (Fig. 3i–l). Pre-incubation with DNase I prior to TUNEL reaction induced DNA cleavage in both small and large cell domains (Fig. 3m–p), whereas no TUNEL signal was found in negative controls when the transferase was omitted in the TUNEL reaction (data not shown).

In order to investigate the time course analysis of DNA degradation, genomic DNA from 1- to 8-day-old

MCSs was extracted and separated by conventional agarose gel electrophoresis. Extensive DNA degradation could be detected on gel in 7-day-old MCSs and 8-day-old ELSs (Fig. 4a). The apparent 2-days delay in detecting DNA fragmentation on gel compared to the detection of TUNEL-positive nuclei indicates that massive cell death takes place around 7–8 days of culture. In order to determine the dynamics of exine wall rupture, the daily frequency of ELSs released out of the exine wall was determined (Fig. 4b, open bars). An average of $50 \pm 1.52\%$ of the ELSs were released out of the exine after 7 days of culture, overlapping with the extensive DNA degradation observed in 7- and 8-day-old cultures (Fig. 4a).

To better understand the events leading to DNA degradation during PCD of the small cell domain, caspase-3-like activity toward the synthetic fluorogenic caspase-3 substrate Ac-DEVD-AMC was assayed (Fig. 4b, black bars). A significant increase of the caspase-3-like activity measured in 1- to 3-day-old MCSs was observed after 4 days of culture ($P < 0.0004$), whereas TUNEL positive nuclei were only detected after 5 days of culture (Fig. 3e–h). The increase in the caspase-3-like activity in 4- and 5-day-old MCSs showed a peak at 6 days of culture ($P < 0.000002$) and significantly decreased thereafter. The peak of the caspase-3-like activity measured in 6-day-old MCSs extracts preceded the DNA degradation observed after 7 days and 8 days of culture (Fig. 4a) and the peak of exine wall rupture in 7-day-old MCSs (Fig. 4b, open bars). The caspase-3-like activity was efficiently inhibited by the specific mammalian caspase-3 inhibitor Ac-DEVD-CHO (Fig. 4b, gray bars). These results suggest that developing barley MCSs contain a caspase-3-like protease or a group of related proteases with the substrate preference and inhibitor specificity similar of mammalian caspase-3.

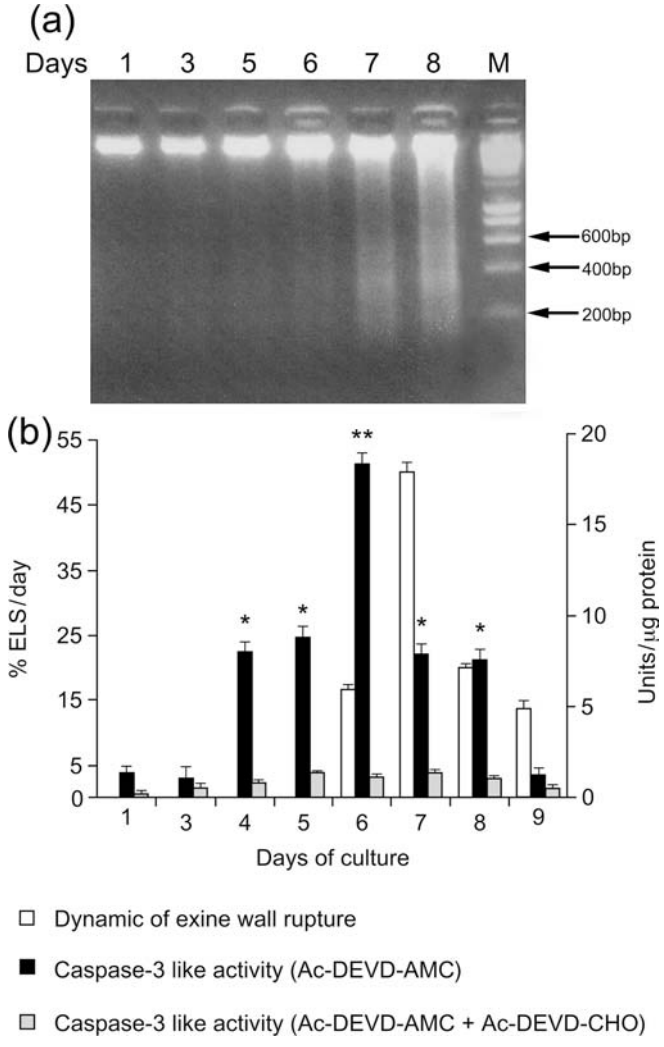

Fig. 4 Time course analysis of DNA degradation, exine wall rupture dynamics and caspase-3-like activity. **a** Conventional DNA gel electrophoresis in 1- to 8-day-old MCSs and ELSs. DNA degradation is observed in 7-day-old MCSs and 8-day-old ELSs. *M*, marker DNA. **b** Dynamics of exine wall rupture (*open bars*) and caspase-3-like activity in total protein extracts of 1- to 9-day-old MCSs and ELSs in liquid culture (*black bars*). * Mean value significantly different than value measured at 1 day of culture ($P < 0.0004$). ** Mean value significantly different from values obtained in all the other samples measured ($P < 0.000002$). Cleavage of the specific animal fluorogenic caspase-3 substrate (Ac-DEVD-AMC) was measured at 460 nm and was efficiently inhibited by the caspase-3 inhibitor (Ac-DEVD-CHO, *gray bars*) ($n = 3$)

Morphology of cell dismantling

Since PCD involves specific cellular changes during cell dismantling, the ultrastructure of cell death was investigated by TEM in MCSs and ELSs around the time of exine wall rupture. One of the most striking differences between the two cellular domains was the electron-dense cytoplasm of the small cells in 5-day-old MCSs prior to exine wall rupture (Fig. 5a). Due to the high density of the cytoplasm, few organelles could be distinguished at this stage. Among these, amyloplasts filled with starch granules, lipid bodies and mitochondria could be recognized. The nucleus showed a very condensed chromatin structure, and the nucleolus was very dense, characteristic of cells with little transcription activity (Fig. 5b). The first ultrastructural change associated with PCD visualized in the nucleus was the formation of patches of condensed chromatin (Fig. 5c), which differed from the regular organized condensed chromatin structure (Fig. 5b). In the cytoplasm, mitochondria became less electron-dense (Fig. 5c). After exine wall rupture in 7-day-old MCSs, osmiophilic bodies were observed near the cell membranes and in the extracellular space of the dying cells, adjacent to the exine wall (Fig. 5d). Following exine wall rupture, the small cells detached from the large cell domain (Fig. 5e). The process of cell detachment occurred in an asynchronous way, since it was possible to identify small cells at different stages of cell dismantling in one ELS (data not shown). During cell detachment, the cell walls surrounding the large cells were not removed, but only the ones surrounding the dying cells (Fig. 5e, indicated by arrows). In advanced stages of cell dismantling, the cytoplasm appeared less electron-dense, mito-

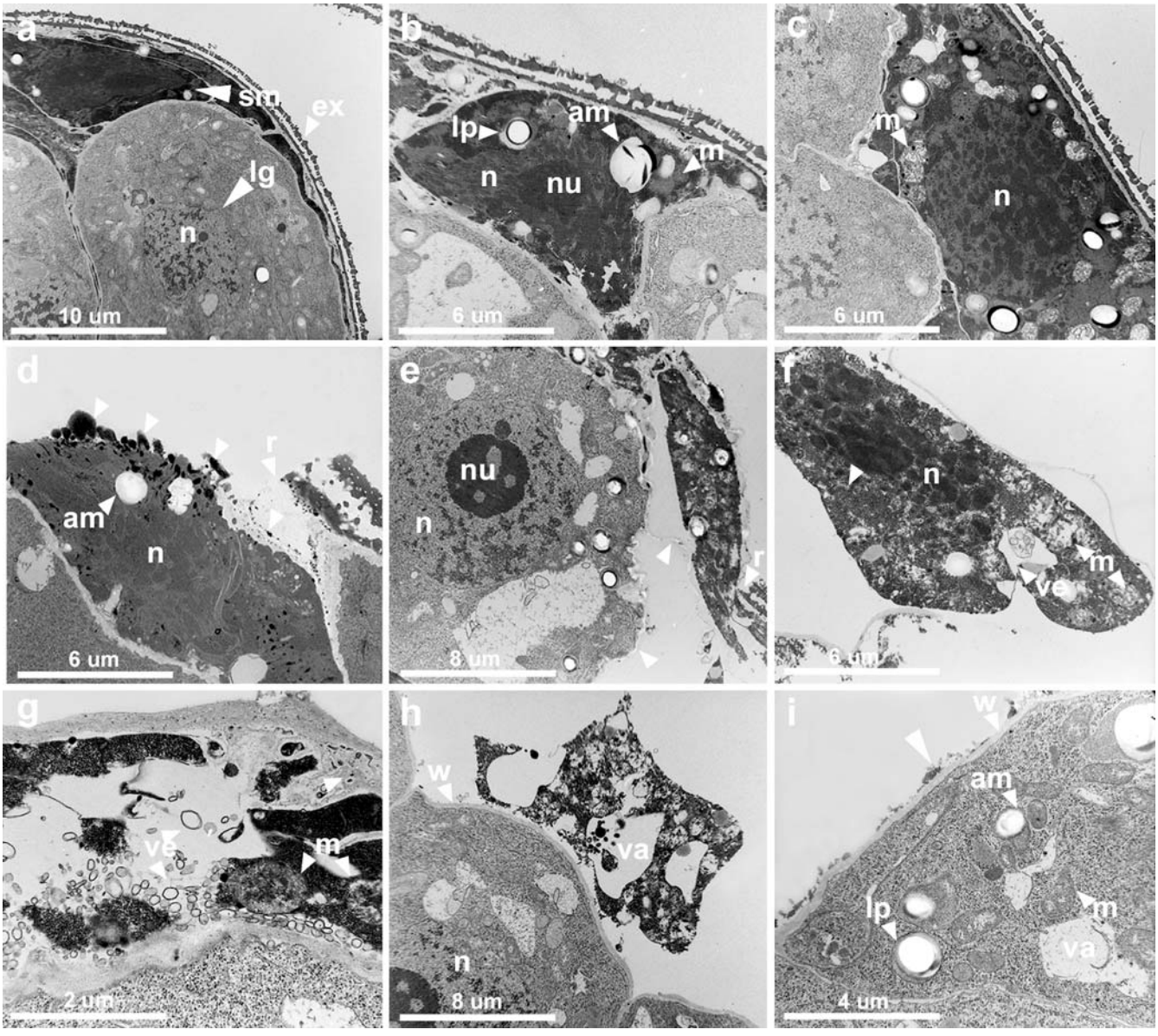

Fig. 5 TEM analysis of PCD in MCSs and ELSs. **a**–**c** Five-day-old MCSs. **a** The cytoplasm of the small cell domain is highly electron-dense compared to the cytoplasm of the large cell domain. **b** A close-up of a small cell illustrates that the cytoplasm of the small cells contains amyloplasts, lipid bodies and mitochondria, while the nucleus shows a high degree of chromatin condensation. **c** The first ultrastructural changes associated with PCD are visualized by the formation of disorganized patches of chromatin in the nucleus and by a decrease in mitochondria electron-density. **d**–**h** Seven-day-old MCSs showing the ultrastructure of the progressive stages of cell dismantling. *Arrows* in **d** indicate osmiophilic bodies while in **e** indicate cell wall detachment. **i** Region of 9-day-old ELS showing large cell domain after elimination of the small cells. *am* Amyloplasts, *ex* exine wall, *lg* large cell domain, *lp* lipid bodies, *m* mitochondrion, *n* nucleus, *nu* nucleolus, *r* exine wall rupture, *sm* small cell domain, *ve* vesicles *va*, vacuole, *w* cell wall

chondria were collapsed and small vesicles were visible. Cytoplasmic material was contained by vesicles and large vacuoles (Fig. 5f–h). Despite the high degree of cytoplasm collapse, the condensed chromatin in the nucleus persisted until later stages of cell dismantling (Fig. 5f). After cell dismantling was completed, cell debris resulting from the disassembly of the small cells remained in contact with the cell wall of the large cell domain in 9-day-old ELSs (Fig. 5i).

The changes in the external morphology of the dividing structures around the time of exine wall rupture were studied by SEM. SEM observations revealed the subsequent stages in exine wall rupture during the transition of MCSs into ELSs (Fig. 6). The first stage was frequently observed after 7 days of culture and represented the rupture of the exine wall at the site of the small cell domain. This rupture generated a crack, exposing the dead small cells to the exine exterior (Fig. 6a). The small cell domain possessed a very compact structure and the cells showed a flattened shape with a smooth surface (Fig. 6a). The second stage in exine wall rupture was often observed in 7- to 9-day-old cultures. In the second stage, cell dis-

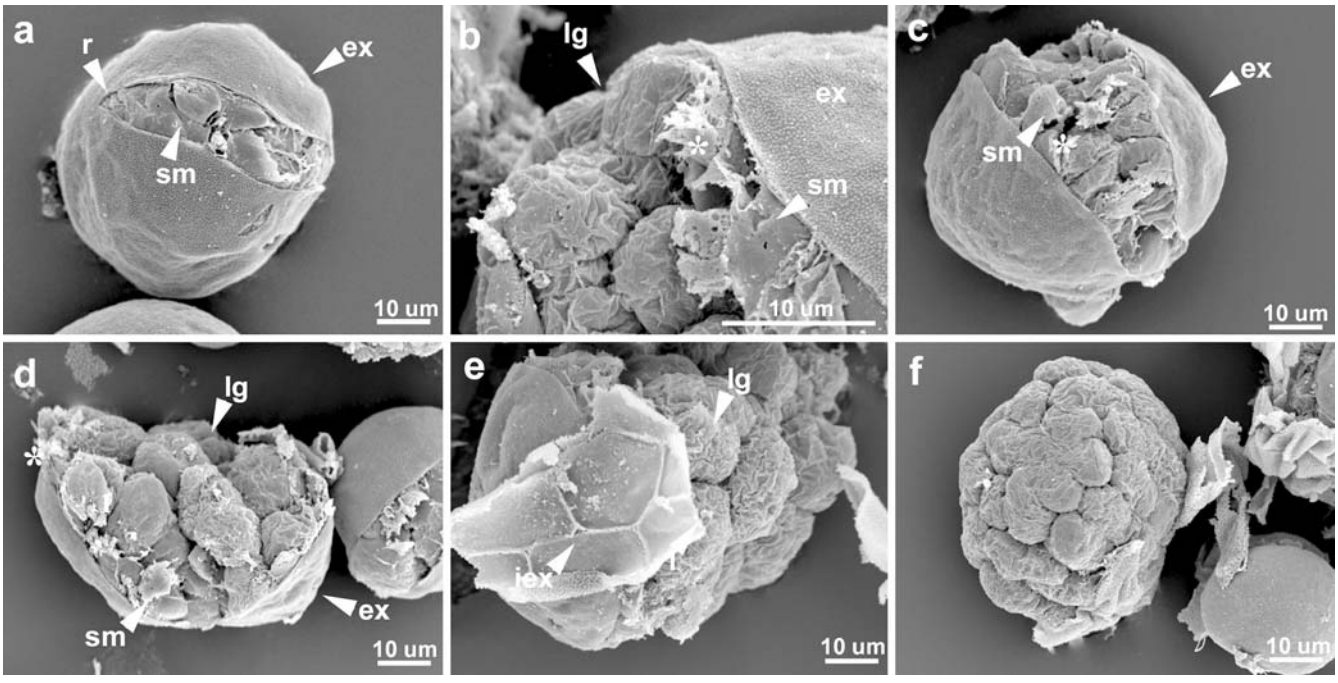

Fig. 6 SEM analysis of MCSs and ELSs illustrating the three stages of exine wall rupture during the transition from MCSs to globular embryos. **a** Stage one, 7-day-old MCSs: rupture of the exine at the site of the small cell domain, exposing the small cells to the exine exterior. **b–d** Stage two, 7- to 9-day-old MCSs: cell dismantling and cell detachment of the small cell domain. Cell debris attached to the edges of the opening exine are marked by (*). **e** Stage three, 9-day-old ELS: exine wall detachment from the large cell domain. **f** 11-day-old ELS after exine wall detachment at the stage of globular embryo. *ex* Exine wall, *iex* inner side of the exine wall, *lg* large cell domain, *r* exine wall rupture, *sm* small cell domain

mantling and cell detachment took place in the small cell domain (Fig. 6b–d). This produced a gap within the small-celled domain, which exposed the large cell domain to the exine exterior. The large cell domain possessed loose structure and the cells showed a round shape with a rough surface (Fig. 6b). While the debris of the small cells remained attached to the edges of the opening exine, the crack in the exine further expanded as the large cells divided (Fig. 6b–d). In the third stage, the exine detached from the large, embryogenic cells. During exine detachment, the continuous and smooth pattern of the outer surface of the exine changed, as it became fragmented by its adhesion to the contours of the large cells (Fig. 6e). After the exine wall was detached from the outer surface of the large-celled domain, 11-day-old ELSs resembled zygotic globular embryos (Fig. 6f).

Discussion

Origin and fate of the two different cellular domains in embryogenic MCSs of barley

Cytological observations during the early stages of barley androgenesis revealed that both symmetric and asymmetric divisions result in the formation of MCSs. Symmetric divisions are characterized by the presence of two vegetative-like nuclei and give rise to homogeneous MCSs. On the other hand, asymmetric divisions lead to the formation of heterogeneous MCSs, characterized by a small cell domain with condensed chromatin structure of nuclei and a large cell domain showing normal chromatin structure of nuclei. The morphology of these nuclei resembles that of generative and vegetative nuclei of developing pollen grains (McCormick 1993). These results indicate that both the B-pathway (Sunderland et al. 1979; Kasha et al. 2001) and the modified version of the A-pathway (Sunderland et al. 1979) contribute to MCS formation during barley androgenesis induced by an anther mannitol treatment. The progression of the embryogenic pathway during the transition of MCSs into ELSs in barley has been reported to occur only from MCSs that display cell death at the site of exine wall rupture (Maraschin et al. 2004). We further demonstrate that cell death takes place in the small cell domain of heterogeneous MCSs, indicating that they represent the embryogenic MCSs previously described (Maraschin et al. 2004). This is the first report to show that heterogeneous MCSs developed via the modified A-pathway are the real embryogenic MCSs that result in the formation of ELSs in barley androgenesis.

The characterization of the events that resulted in the formation of heterogeneous MCSs indicates that the generative cell divides to give rise to a small cellular domain localized at the opposite side of the pollen germ pore. Cell tracking experiments have shown that the first divisions in embryogenic MCSs of barley take place at the opposite side of the pollen germ pore (Bolik and Koop 1991; Kumlehn and Lörz 1999; Maraschin et al. 2004). These findings suggest that the early stages of

microspore embryogenesis in barley are marked by the divisions of the generative cell rather than the vegetative cell, which was shown to divide later. In barley, such division patterns have been reported to give rise to heterogeneous MCSs that have been termed 'partitioned units', to denote MCSs composed of different cellular types (Sunderland et al. 1979). Due to the compact cellular organization of the generative domain and the initial free nuclear divisions of the vegetative domain, these domains have been compared to the embryo and endosperm initials in zygotic embryogenesis (Sunderland and Huang 1985). More recently, embryogenic and endosperm domains have been also described among wheat and maize MCSs (Bonet and Olmedilla 2000; Magnard et al. 2000). Despite the similarities shared between the small and large cell domains described in the present work and the embryogenic and endosperm initials described previously (Sunderland et al. 1979; Sunderland and Huang 1985), we show that the small cell domain is eliminated during the process of exine wall rupture and does not contribute to embryo formation, whereas the large cell domain gives rise to ELSs. By SEM, the morphology of ELSs released out of the exine wall resembles that of globular embryos, which showed no apparent signs of pattern formation. Our previous results have shown that pattern formation arises later in culture, when globular embryos released out of the exine wall acquire bilateral symmetry (Maraschin et al. 2003). The expression of the 14-3-3C isoform, a member of the conserved family of 14-3-3 regulatory proteins, has been reported to mark scutellum development during this process (Maraschin et al. 2003). These results indicate that pattern formation is probably not due to the different cellular domains present in MCSs contained within the exine as previously proposed (Sunderland et al. 1979; Sunderland and Huang 1985). It appears more likely that pattern formation arises after exine wall rupture in globular embryos, a process that might involve new developmental cues.

PCD during the transition from MCSs to globular embryos

During development, uses of PCD include the formation of the plant body plans and specific organ shapes and the removal of unwanted or damaged cells. Three main cytological variants of PCD have been identified in plants (Fukuda 2000). In apoptotic-like cell death, a process that is analogous to apoptosis in animal PCD, chromatin condensation, nuclear shrinkage and fragmentation, and DNA laddering are known to precede cytoplasm degradation (Pennel and Lamb 1997). Though this appears to be the classical type of PCD during hypersensitive response and anther tapetum degeneration (Fukuda 2000; Wang et al. 1999), during the differentiation of tracheary elements it is the vacuolar collapse that precedes nuclear DNA fragmentation (Obara et al. 2001). A third type of cell-death morphology has been described within pro-embryos and suspensor cells during somatic embryogenesis of Norway spruce (*Picea abies* L. Karst). In this case, PCD showed apoptotic features concomitantly to autophagy, which was marked by the engulfment of cytoplasmic contents (Filonova et al. 2000).

The morphology of the small cells eliminated by PCD during exine wall rupture presents unique characteristics. Prior to exine wall rupture, the cytoplasm of the small cells is very dense, whereas the nucleus shows condensed chromatin structure. Condensation of nuclear chromatin and an electron-dense cytoplasm have been pointed as morphological markers of plant PCD (Pennel and Lamb 1997; Domínguez et al. 2001; Aleksandrushkina et al. 2004). However, in the small cell domain of barley MCSs, these characteristics appear to be inherent to their generative cell origin rather than induced by PCD, since they were observed prior to any PCD event had started. The first morphological changes associated with PCD in the nucleus are DNA degradation and the aggregation of chromatin into disorganized patches; however, condensed chromatin did not appear marginalized in the nuclear envelope like during pyknosis in most plant PCD events (Pennel and Lamb 1997). In the cytoplasm, mitochondria became less electron-dense, an indication of mitochondria collapse (Ku et al. 2003). At the exine wall rupture site, osmiophilic bodies were present near the cell membranes and in the extracellular space of the small cells, a morphology that preceded cell detachment and subsequent cytoplasm dismantling. During the PCD events leading to leaf shape remodeling and nucellus degeneration, osmiophilic bodies have been reported near the cell membrane and tonoplast, and in the extracellular space prior to cytoplasm disassembly (Domínguez et al. 2001; Gunawardena et al. 2004). Though the identity of the vesicles heavily stained by osmium has not been identified yet, evidence points out that their presence marks the initiation of the events leading to cytoplasm dismantling during plant PCD.

A remarkable feature of the small dying cells is their detachment from the large cell domain after exine wall rupture. Cell detachment is a characteristic of PCD in the root cap of a wide range of plant species and it is also present during cell death in somatic embryogenic cultures of carrot (*Daucus carota* L.) (Pennel and Lamb 1997; Willats et al. 2004). After detachment of the small cells from the large cell domain, cell dismantling is characterized by the presence of vesicles and large vacuoles that contain cytoplasmic material. The sequence of events during cytoplasm dismantling in the small cell domain appears to have similarities to the apoptotic-autophagic morphology described during somatic embryogenesis of Norway spruce (Filonova et al. 2000). Apoptotic-autophagic plant PCD is analogous to the cytoplasmic degenerative morphotype of animal PCD, where cell death takes place *en masse*, as in the elimination of undesired tissues or complete organs,

suggesting overlapping mechanisms of PCD across animal and plant kingdoms (Jones 2000).

During apoptosis, the most studied case of animal PCD, the first irreversible step in the initiation of the cell death program is the activation of a proteolytic cascade involving caspase proteases. Despite the absence of canonical caspases in plants, dying cells have been reported to have increased proteolytic activities for caspase-1, −3 and −6 (Lam and del Pozo 2000; Bozhkov et al. 2004). The apparent diversity in the different caspase-like proteases required for PCD in plants is in agreement with their role in animal PCD, since the death of specific cell types and diverse stimuli have been reported to involve different sets of caspases (Raff 1998). Nevertheless, the most prevalent executioner caspase in animal cells has been pointed to be caspase-3 (Thornberry and Lazebnik 1998). To date, no plant protease displaying caspase-3-like activity has been so far purified. Recent efforts to purify and characterize the proteases responsible for the caspase-like activities in plant cells has indicated that serine proteases and a vacuolar processing enzyme, which is a cysteine protease, might potentially account for the caspase-like activities upon plant PCD (Coffeen and Wolpert 2004; Hatsugai et al. 2004). These results suggest that different plant proteases with similar substrate and inhibitor properties of the mammalian caspase-3 might be active during PCD in barley MCSs.

Following activation of the caspase cascade in animal cells, the DNA in the nucleus is cleaved into 180 bp fragments by a caspase-activated DNase (Enari et al. 1998; Sakahira et al. 1998). Upon plant PCD, caspase-like activity has been reported to precede DNA laddering (Lam 2004), and several DNases have been implicated in this process (Mitler and Lam 1997; Stein and Hansen 1999). Though no caspase-activated DNases have been so far identified in plants, the DNA degradation observed during PCD followed the peak of caspase-3-like activity in barley MCSs. This sequence of events points to a possible role of caspase-3-dependent PCD in executing exine wall rupture. Additional roles for the elimination of the small generative cells by PCD might be associated with sculpting of the microspore embryos, as caspase-6-dependent PCD has been recently demonstrated to be essential for correct embryo pattern formation during in vitro somatic embryogenesis in Norway spruce (Bozhkov et al. 2004). The characterization of the molecular events leading to PCD in barley androgenesis will help establishing a causal relation between PCD and exine wall rupture and will shed light on the mechanisms involved in plant PCD regulation. In this regard, biotechnological applications of PCD may be envisaged, since regulation of the PCD processes that take place during microspore and somatic embryogenesis may provide new tools for the manipulation of quality and yield of in vitro-developed plant embryos.

Acknowledgements We are grateful to Dr. Wessel de Priester (Institute of Biology Leiden, Leiden University, The Netherlands) for valuable discussion and critical reading of the manuscript and to Peter Hock for the layout of the figures.

References

Aleksandrushkina NI, Zamyatnina VA, Bakeeva LE, Seredina AV, Smirnova EG, Yaguzhinsky LS, Vanyushin BF (2004) Apoptosis in wheat seedlings grown under normal daylight. Biochemistry (Mosc) 69:285–294

Bolik M, Koop HU (1991) Identification of embryogenic microspores of barley (*Hordeum vulgare* L.) by individual selection and culture and their potential for transformation by microinjection. Protoplasma 162:61–68

Bonet FJ, Olmedilla A (2000) Structural changes during early embryogenesis in wheat pollen. Protoplasma 211:94–102

Bozhkov PV, Filonova LH, Suarez MF, Helmersson A, Smertenko AP, Zhivotovsky B, von Arnold S (2004) VEIDase is a principal caspase-like activity involved in plant programmed cell death and essential for embryonic pattern formation. Cell Death Differ 11:175–182

Coffeen WC, Wolpert TJ (2004) Purification and characterization of serine proteases that exhibit caspase-like activity and are associated with programmed cell death in *Avena sativa*. Plant Cell 16:857–873

Domínguez F, Moreno J, Cejudo FJ (2001) The nucellus degenerates by a process of programmed cell death during the early stages of wheat grain development. Planta 213:352–360

Enari M, Sakahira H, Yokoyama H, Okawa K, Iwamatsu A, Nagata S (1998) A caspase-activated DNase that degrades DNA during apoptosis, and its inhibitor ICAD. Nature 391:43–50

Filonova LH, Bozhkov PV, Brukhin VB, Daniel G, Zhivotovsky B, von Arnold S (2000) Two waves of programmed cell death occur during formation and development of somatic embryos in the gymnosperm, Norway spruce. J Cell Sci 113:4399–4411

Fukuda H (2000) Programmed cell death of tracheary elements as a paradigm in plants. Plant Mol Biol 44:245–253

Gunawardena AHLAN, Greenwood JS, Dengler NG (2004) Programmed cell death remodels lace plant shape during development. Plant Cell 16:60–73

Hatsugai N, Kuroyanagi M, Yamada K, Meshi T, Tsuda S, Kondo M, Nishimura M, Hara-Nishimura I (2004) A plant vacuolar protease, VPE, mediates virus-induced hypersensitive cell death. Science 305:855–858

Hoekstra S, van Zijderveld MH, Louwerse JD, Heidekamp F, van der Mark F (1992) Anther and microspore culture of *Hordeum vulgare* L. cv. Igri. Plant Sci 86:89–96

Hoekstra S, van Zijderveld MH, Heidekamp F, van der Mark F (1993) Microspore culture of *Hordeum vulgare* L.: the influence of density and osmolarity. Plant Cell Rep 12:661–665

Huang B (1986) Ultrastructural aspects of pollen embryogenesis in *Hordeum*, *Triticum*and *Paeonia*. In: Hu H, Hongyuan Y (eds) Haploids of higher plants in vitro. Springer, Berlin Heidelberg New York, pp 91–117

Indrianto A, Barinova I, Touraev A, Heberle-Bors E (2001) Tracking individual wheat microspores in vitro: identification of embryogenic microspores and body axis formation in the embryo. Planta 212:163–174

Jones A (2000) Does the plant mitochondrion integrate cellular stress and regulate programmed cell death? Trends Plant Sci 5:225–229

Kasha KJ, Hu TC, Oro R, Simion E, Shim YS (2001) Nuclear fusion leads to chromosome doubling during mannitol pretreatment of barley (*Hordeum vulgare* L.) microspores. J Exp Bot 52:1227–1238

Kim M, Kim J, Yoon M, Choi DI, Lee KM (2004) Origin of multicellular pollen and pollen embryos in cultured anthers of pepper (*Capsicum annum*). Plant Cell Tissue Organ 77:63–72

Korthout HAAJ, Berecki G, Bruin W, van Duijn B, Wang M (2000) The presence and subcellular localization of caspase 3-like proteinases in plant cells. FEBS Lett 475:139–144

Ku S, Yoon H, Suh HS, Chung YY (2003) Male-sterility of thermosensitive genic male- sterile rice is associated with premature programmed cell death of the tapetum. Planta 217:559–565

Kumlehn J, Lörz H (1999) Monitoring sporophytic development of individual microspores of barley (*Hordeum vulgare* L.). In: Clement C, Pacini E, Audran JC (eds) Anther and pollen: from biology to biotechnology. Springer, Berlin Heidelberg New York, pp 183–189

Lam E (2004) Controlled cell death, plant survival and development. Nat Rev Mol Cell Biol 5:305–315

Lam E, del Pozo O (2000) Caspase-like protease involvement in the control of plant cell death. Plant Mol Biol 44:417–428

Magnard JL, Le Deunff E, Domenech J, Rogowsky PM, Testillano PS, Rougier M, Risueño MC, Vergne P, Dumas C (2000) Genes normally expressed in the endosperm are expressed at early stages of microspore embryogenesis in maize. Plant Mol Biol 44:559–574

Maraschin SF, Lamers GEM, de Pater BS, Spaink HP, Wang M (2003) 14–3-3 isoforms and pattern formation during barley microspore embryogenesis. J Exp Bot 51:1033–1043

Maraschin SF, Vennik M, Lamers GEM, Spaink HP, Wang M (2004) Time-lapse tracking of barley androgenesis reveals position-determined cell death within pro-embryos. Planta (in press)

McCormick S (1993) Male gametophyte development. Plant Cell 5:1265–1275

Mitler R, Lam E (1997) Characterization of nuclease activities and DNA fragmentation induced upon hypersensitive response cell death and mechanical stress. Plant Mol Biol 34:209–221

Mordhorst AP, Toonen MAJ, de Vries SC (1997) Plant embryogenesis. Crit Rev Plant Sci 16:535–576

Obara K, Kuriyama H, Fukuda H (2001) Direct evidence of active and rapid nuclear degradation triggered by vacuole rupture during programmed cell death in Zinnia. Plant Physiol 125:615–626

Pennel RI, Lamb C (1997) Programmed cell death in plants. Plant Cell 9:1157–1168

Pretova A, de Ruijter NCA, van Lammeren AAM, Schel JHN (1993) Structural observations during androgenic microspore culture of the 4c1 genotype of *Zea mays* L. Euphytica 65:61–69

Raff M (1998) Cell suicide for beginners. Nature 396:119–122

Raghavan V (1986) Pollen embryogenesis. In: Barlow PW, Green PB, Wylie CC (eds) Embryogenesis in angiosperms. Cambridge University Press, Cambridge, pp 153–189

Sakahira H, Enari M, Nagata S (1998) Cleavage of CAD inhibitor in CAD activation and DNA degradation during apoptosis. Nature 391:96–99

Stein JC, Hansen G (1999) Mannose induces an endonuclease responsible for DNA laddering in plant cells. Plant Physiol 121:71–79

Sunderland N (1974) Anther culture as a means of haploid induction. In: Kasha KJ (ed) Haploids in higher plants: advances and potential. University of Guelph, Canada, pp 91–122

Sunderland N, Evans LJ (1980) Multicellular pollen formation in cultured barley anthers. II. The A, B and C pathways. J Exp Bot 31:501–514

Sunderland N, Huang B (1985) Barley anther culture—the switch of programme and albinism. Hereditas 3:27–40

Sunderland N, Roberts M, Evans LJ, Wildon DC (1979) Multicellular pollen formation in cultured barley anthers. I. Independent division of the generative and vegetative cells. J Exp Bot 30:1133–1144

Thornberry NA, Lazebnik Y (1998) Caspases: enemies within. Science 281:1312–1316

Touraev A, Pfosser M, Vicente O, Heberle-Bors E (1996) Stress as the major signal controlling the developmental fate of tobacco microspores: towards a unified model of induction of microspore/pollen embryogenesis. Planta 200:144–152

Touraev A, Vicente O, Heberle-Bors E (1997) Initiation of microspore embryogenesis by stress. Trends Plant Sci 2:297–302

Říhová L, Tupý J (1999) Manipulation of division symmetry and developmental fate in cultures of potato microspores. Plant Cell Tissue Organ 59:135–145

Vergne P, Delvallee I, Dumas C (1987) Rapid assessment of microspore and pollen development stage in wheat and maize using DAPI and membrane permeabilization. Stain Technol 62:299–304

Wang M, Hoekstra S, van Bergen S, Lamers GEM, Oppedijk BJ, van der Heijden MW, de Priester W, Schilperoort RA (1999) Apoptosis in developing anthers and the role of ABA in this process during androgenesis in *Hordeum vulgare* L. Plant Mol Biol 39:489–501

Wang M, van Bergen S, van Duijn B (2000) Insights into a key developmental switch and its importance for efficient plant breeding. Plant Physiol 124:523–530

Willats WGT, McCartney L, Steele-King CG, Marcus SE, Mort A, Huisman M, van Alebeek GJ, Schols HA, Voragen AGJ, Le Goff A, Bonnin E, Thibault JF, Knox JP (2004) A xylogalacturonan epitope is specifically associated with plant cell detachment. Planta 218:673–681

Zaki MAM, Dickinson HG (1991) Microspore-derived embryos in *Brassica*: the significance of division symmetry in pollen mitosis I to embryogenic development. Sex Plant Rep 4:48–55